A Linearized Optical Directional-Coupler Modulator at 1.3 μm

Chanin Laliew, Sigurd Weidemann Løvseth, Xiaobo Zhang, and Anand Gopinath, *Fellow, IEEE*

***Abstract*—We investigate electrooptic directional-coupler modulators operating at the wavelength of 1.3 μm, to have high linearity in their response function. The inverse Fourier transform technique was used to synthesize the spatially varying coupling function from a specified response function. The resulting coupling function was then used to determine the shape of the modulator structure. Modulators to have the response function of the form of a triangular ("linear") function have been designed, fabricated, and tested. The third-order intermodulation-limited spurious-free dynamic range, at −130-dBm normalized noise floor, of 96.2 dB/Hz$^{2/3}$ was obtained.**

***Index Terms*—Directional-coupler modulator, electrooptic modulator, linearized modulator, spatially varying coupling function.**

I. Introduction

DURING the past decade there has been a rapidly growing interest in analog transmission over the fiber-optic medium. The main interest for these investigations and experiments has been shown for microwave applications and cable-TV distribution. For these applications, an external optical modulator is a necessary device as directly modulating the optical source leads to spectral broadening, and hence reducing the available bandwidth of the optical communication system. Several different types of optical modulators may be used, including the electroabsorption and the electrooptic modulators. In this paper we only consider the electrooptic modulators. Two types of electrooptic modulators are commonly used : the Mach–Zehnder interferometric type and the directional coupler type. The basic Mach–Zehnder interferometric modulator has a squared-cosine response function (the dependence of the amplitude-modulated optical power on the applied voltage) and the basic uniform directional coupler modulator has a quasi-squared-sinc response function, both of which are highly nonlinear, and to avoid crosstalk this leads to a use of relatively low modulation index of about 2%–5% in currently available optical modulators. Therefore, there have been attempts to find external optical modulators which would provide much better linearity in their response functions so that the system capacity can be maximally utilized. A variety of linearization concepts have been proposed, and the goal of which is either to adjust the response function to fit a linear function or to eliminate or suppress the cubic and/or higher order terms in Taylor expansion of the response function. This gives rise to a variety of device configurations used, ranging from the simple Mach–Zehnder interferometer [1], dual-parallel Mach–Zehnder interferometer [2], modified directional coupler [3], and a combination of Mach–Zehnder interferometer and directional coupler [4]–[6]. In our work, we design electrooptic modulators from directional couplers, but instead of the coupler having a pair of waveguides running in parallel, i.e., having a constant or uniform coupling, we design them so that the spacing between the two waveguides varies along the length of the device structure, and the response function is then of the desired form. This is the first time a linearized electrooptic modulator built from a directional coupler with a spatially varying coupling function result is obtained experimentally.

In this paper we discuss how the spatially varying coupling function may be synthesized from a specified response function, and then the modulator design and the experimental results of the fabricated modulators are given. We first give some background discussion on the theory of the waveguide directional coupler for completeness.

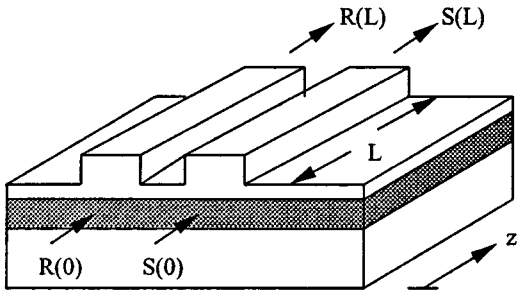

Fig. 1. Schematic diagram of a directional coupler.

II. Waveguide Directional Coupler

A. Coupled-Mode Theory

A typical waveguide directional coupler is schematically shown in Fig. 1. Here two waveguides are brought in close proximity with each other over an interaction length L, and coupling occurs between the optical modes of the two waveguides via their evanescent fields. The coupling action may be described by the well-known coupled-mode equations [7]:

$$\frac{dR(z)}{dz} = j\delta R(z) - j\kappa(z)S(z)e^{-j\phi(z)} \tag{1a}$$

$$\frac{dS(z)}{dz} = -j\delta S(z) - j\kappa(z)R(z)e^{-j\phi(z)} \tag{1b}$$

where $R(z)$ and $S(z)$ represent the complex amplitudes of the two coupled modes. In this representation, $R(z)$ and $S(z)$ are

Manuscript received July 9, 1999; revised May 2, 2000. This work was supported by DARPA and the U.S. Air Force.

The authors are with the Department of Electrical and Computer engineering, University of Minnesota, Minneapolis, MN 55455 USA (e-mail: claliew@ece.umn.edu).

Publisher Item Identifier S 0733-8724(00)08072-5.

normalized such that the condition $|R(z)|^2 + |S(z)|^2 = 1$ is satisfied, according to the law of conservation of energy in the system. $\kappa(z)$ is called the coupling coefficient and $\delta = \Delta\beta/2$, with $\Delta\beta$ being the difference between the propagation constants of the optical modes in the individual waveguides as if they were isolated, and $\phi(z)$ is defined as

$$\phi(z) = \int_0^z [\Delta\beta(z') - \Delta\beta(0)]\, dz'. \tag{2}$$

Note that for uniform directional couplers, $\kappa(z)$ becomes a constant and $\phi(z) = 0$.

For *uniform* directional couplers with the initial condition that if we inject light of unit amplitude to the input of one waveguide, but not to the other, i.e., $R(0) = 1$ and $S(0) = 0$, the solutions to the coupled-mode equations (1a) and (1b) are given by [8]

$$S(z) = -j\kappa \frac{\sin\left(z\sqrt{\kappa^2 + \delta^2}\right)}{\sqrt{\kappa^2 + \delta^2}} \tag{3}$$

$$R(z) = \cos\left(z\sqrt{\kappa^2 + \delta^2}\right) + j\delta \frac{\sin\left(z\sqrt{\kappa^2 + \delta^2}\right)}{\sqrt{\kappa^2 + \delta^2}}. \tag{4}$$

The coupling efficiency η defined as the intensity of light in the guide that initially was not excited if the other guide was excited with unit intensity then becomes

$$\eta \equiv |S(z)|^2_{R(0)=1,\, S(0)=0} = \frac{\sin^2\left(\kappa z\sqrt{1 + (\delta/\kappa)^2}\right)}{1 + (\delta/\kappa)^2}. \tag{5}$$

When a pair of electrodes are introduced on top of the waveguides and voltages are applied, δ will change accordingly (via the linear electrooptic effect). By this means, the directional coupler can be used as a modulator, and $\eta(\delta)$ is termed the "response function," or simply "response," of the modulator. Referring to (5), we see that the response function of a modulator built from a uniform directional coupler is highly nonlinear. However, it is possible to construct a directional-coupler modulator with a response that differs dramatically from that of a uniform directional-coupler modulator, by spatially varying the coupling function by means of a synthesis technique to obtain a specified response function. In our project, we used the inverse Fourier transform technique to render directional-coupler modulators that have high linearity in their response function. Details of this method will be discussed in Section III.

B. The Riccati Equation in the Coupled-Mode Theory

From the coupled set of linear differential equations (1a) and (1b), it is possible to derive the nonlinear Riccati differential equation with only one dependent variable [9]. The starting point is to define the dependent variable ρ as

$$\rho = \frac{S}{R} e^{-j\phi(z)}. \tag{6}$$

By straightforward differentiation of ρ with respect to z, we get

$$\frac{\partial\rho}{\partial z} = \left(\frac{\frac{\partial S}{\partial z}}{R} - \frac{S\frac{\partial R}{\partial z}}{R^2} - j\frac{S\frac{\partial\phi}{\partial z}}{R}\right) e^{-j\phi(z)}. \tag{7}$$

Inserting (1a) and (1b) into (7), and using the definition of ρ as given in (6), the Riccati equation

$$\frac{\partial\rho}{\partial z} = -j\left(2\delta + \frac{\partial\phi}{\partial z}\right)\rho + j\kappa(\rho^2 - 1) \tag{8}$$

is thus obtained.

Also, from the definition of ρ given in (6), it follows that the squared amplitude of S is given by

$$\eta = |S|^2 = \frac{|\rho|^2}{1 + |\rho|^2} \tag{9}$$

as $|R|^2 + |S|^2 = 1$ according to the law of conservation of energy in the system.

III. The Inverse Fourier Transform Synthesis Technique

Although it is possible in theory to design a directional-coupler modulator to have a specified response by using the so-called Gel'fand–Levitan–Marchenko inverse scattering method [10]–[12], which gives the exact result, the response function to be used in this method strictly needs to be confined to a certain class of rational polynomial functions, which may not describe the response that we want. Therefore, we have investigated the use of Fourier transform approximation method for directional couplers, initially proposed by Alferness [9], and subsequently used by Winick for the corrugated optical coupler filters [13]. Many authors [9], [13]–[15] have stated that if the energy coupled over from the original dominant mode to the other mode is small, the behavior of the energy transfer between the two coupled waveguides may then be characterized by the Fourier transform of the coupling (function) between them. This can be shown by making the following substitution of ρ in the Riccati equation:

$$\rho = \sigma e^{-j(2\delta z + \phi)}. \tag{10}$$

If it is assumed that negligible coupling has taken place, the absolute value of ρ, and thus σ, is small, the Riccati equation then reduces to

$$\frac{\partial\sigma}{\partial z} \approx -j\kappa e^{j(2\delta z + \phi)}. \tag{11}$$

Since for weak coupling, $\eta = |S|^2 \approx |\rho|^2 = |\sigma|^2$ [see (9) and (10)], by integration, we obtain

$$\eta = |S|^2 \approx \left|\int_{-L/2}^{L/2} \kappa(z) e^{j(2\delta z + \phi)}\, dz\right|^2. \tag{12}$$

Then it follows that

$$S(\delta) = |S(\delta)| e^{j\gamma(\delta)} \approx \int_{-L/2}^{L/2} \kappa(z) e^{j(2\delta z + \phi)}\, dz. \tag{13}$$

In this case, we choose $z = 0$ at the center of the coupler and L is the length of the device. Here $\gamma(\delta)$, which is the phase of $S(\delta)$, is a real function, and it can be shown that $\gamma = -\delta L$ from (3), (4), and (10). Since we have $\kappa = 0$ outside the coupler, the boundaries of the integral can be extended to infinity and we

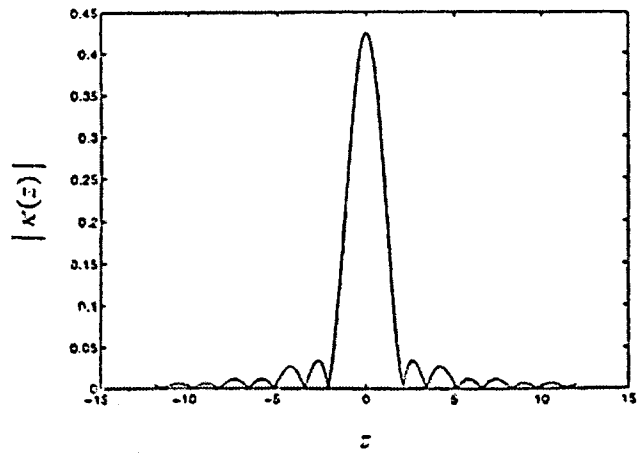

Fig. 2. The absolute value of the spatially varying coupling function $\kappa(z)$ that results when using the Fourier transform method with a response function that ideally should be triangular or linear: $\eta = 1 - |\delta|$.

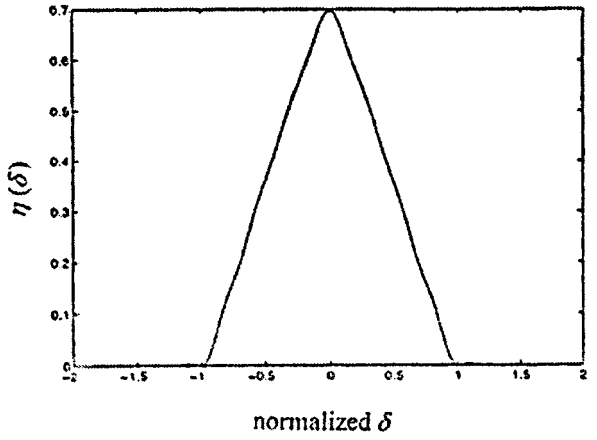

Fig. 3. Response of the modulator having the coupling function shown in Fig. 2.

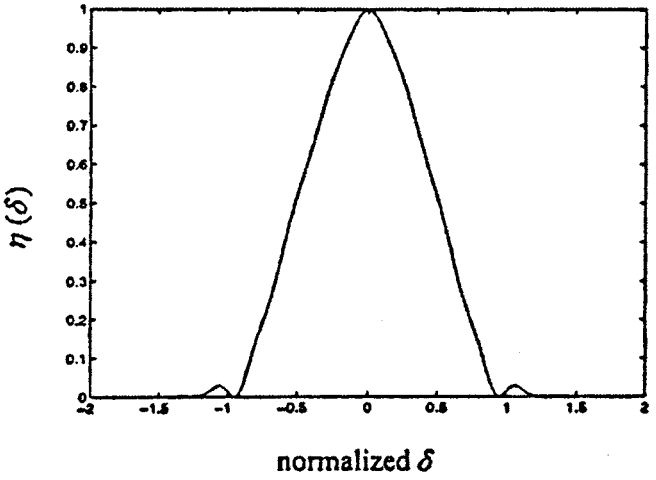

Fig. 4. Response of the modulator having the coupling function scaled so that the maximum efficiency is 100%.

have a Fourier transform of $\kappa e^{j\phi}$ with 2δ as the Fourier "frequency" parameter. It should be pointed out that the usefulness of this approach in our case would be limited since it assumes that $\rho \ll 1$, but when we have complete transfer of energy from one guide to the other, $\rho = \infty$, and even with only 50% energy transfer, $\rho = 1$! Nevertheless, we will still continue to use this approach to find the $\kappa(z)$function. By performing an inverse Fourier transform of (13), we find

$$\kappa(z) = \frac{1}{\pi}\int_{-\infty}^{\infty} |S(\delta)| e^{-j\delta(L+2z)}\, d\delta. \tag{14}$$

Notice that we have multiplied the usual inverse Fourier transform by 2 since it is 2δ, and not δ, that is the Fourier transform variable. In our case, we want $|S(\delta)|$ to be an even function, (14) then reduces to

$$\kappa(z) = \frac{2}{\pi}\int_{0}^{\infty} |S(\delta)| \cos\delta(L+2z)\, d\delta. \tag{15}$$

Thus $\kappa(z)$ becomes the desired coupling function. The Fourier transform of (14) may easily be calculated using fast Fourier transform (FFT) techniques, or if the $|S(\delta)|$ function is nonzero in a limited range, we may find $\kappa(z)$ through direct integration of (15). In our case, we use the ideal linear (triangular) $S(\delta)$ function given by

$$|S(\delta)| = \begin{cases} \sqrt{1-|\delta|}, & |\delta| \le 1 \\ 0, & |\delta| > 1. \end{cases} \tag{16}$$

The device length L is a rather artificial quantity when finding the coupling distribution, and it may be eliminated by shifting the zero point of z. It is then sufficient to calculate

$$\kappa(z) = \frac{2}{\pi}\int_{0}^{1} \sqrt{1-|\delta|}\cos(2\delta z) d\delta. \tag{17}$$

The resulting κ function is shown in Fig. 2, and the calculated response from this κ function is shown in Fig. 3 and is symmetric as anticipated. Quite surprisingly, even though we have used a rather simple approximation method, the shape of the response curve is almost as we wanted it, but maximum coupling efficiency at $\delta = 0$ is only 0.7—this is probably because this approximation is poorest for high coupling efficiency. It may be shown that 100% coupling efficiency at $\delta = 0$ occurs when the integrated value of $\kappa(z)$ over the interaction length is $\pi/2$. However, when we scale the κ function so that this becomes true, the linearity of the resulting response function, as shown in Fig. 4, is not as good as that of the unscaled case.

Note also that at each null in the spatially varying coupling function $\kappa(z)$ we get a sign shift. A negative coupling is in itself meaningless but it may be interpreted that in fact a sign shift in the coupling function corresponds to a phase shift between the two modes by an amount π, and for waveguides made from GaAs at the optical wavelength of 1300 nm, this can be easily achieved in the real directional-coupler structure by adding an extra length of 0.18 μm of one waveguide relative to the other.

IV. Design of the Modulators

We are interested in building directional-coupler modulators which have an ideal linear-function response of the form given in (16). The coupling function corresponding to this response can be obtained using the synthesis technique discussed in the previous section. In our modulator design, the shape of the structure is determined by the ideal theoretically calculated coupling function truncated at the third null, as this gives the response

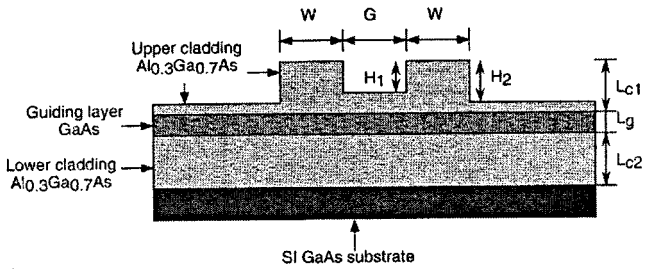

Fig. 5. Cross section of a double-ridge waveguide structure.

function close to that obtained from the full coupling function [16], since the coupling function $\kappa(z)$ rapidly converges toward zero. Depending on where we truncate the coupling function, the response function $\eta(z)$ will always differ from the original specification; the more lobes in the coupling function used, the closer the response function will get to the ideal case. We design the modulator structures so that they are one "coupling length" long, and for the maximum 100% coupling efficiency the relation between the truncated coupling function $\kappa(z)|_{\text{truncated}}$ and the coupling length L_c must obey [14]

$$\int_{-L_c/2}^{L_c/2} \kappa(z)|_{\text{truncated}}\, dz = \frac{\pi}{2} \tag{18}$$

with the center of the device placed at $z = 0$. This maximum efficiency requirement will result in a small loss of linearity of the response function, strictly around $\delta = 0$, however, as seen in Fig. 4. It should be noted also that as the coupling varies along the length of the device, the electrooptically induced phase shift δ will also vary. Therefore, in designing the real device structure we need to locally scale the coupling coefficient κ so that the *ratio* between κ and the electrooptically induced phase shift δ is the same as that of the simulated ideal case, in which the phase shift δ is constant over the whole length of the device.

The cross section of a double-ridge waveguide directional-coupler structure built from the $Al_{0.3}Ga_{0.7}As$/GaAs material system is schematically shown in Fig. 5.

We use the $Al_{0.3}Ga_{0.7}As$/GaAs material system because it shows quite effective electrooptic effect [17] and monolithically integrating it with other semiconductor photonic components is feasible. GaAs and $Al_{0.3}Ga_{0.7}As$ have almost the same lattice constant and both are optically isotropic and are transparent at the wavelength of 1.3 μm. Referring to Fig. 5, we used a fixed value of $L_{c1} = 1$ μm, $L_g = 0.6$ μm, $L_{c2} = 3$ μm, $W = 3$ μm, $H_1 = 0.75$ μm, and $H_2 = 0.85$ μm, and used a computer program [18] to find the effective indices of the TE even and odd "supermodes" in the double-ridge waveguide structure with various interridge gaps G. In our design, we used $H_1 > H_2$, which implies that the outer sidewall is etched deeper than the interridge-gap sidewall; this results in higher coupling between the two guided modes than the case where $H_1 = H_2$ [19].

Fifteen different values of G were used and the effective indices of the even and the odd supermodes were found for each value of G. The coupling coefficient κ corresponding to each interridge gap G can be determined by using the relation [20]

$$\kappa = \frac{\pi}{\lambda}(n_e - n_o) \tag{19}$$

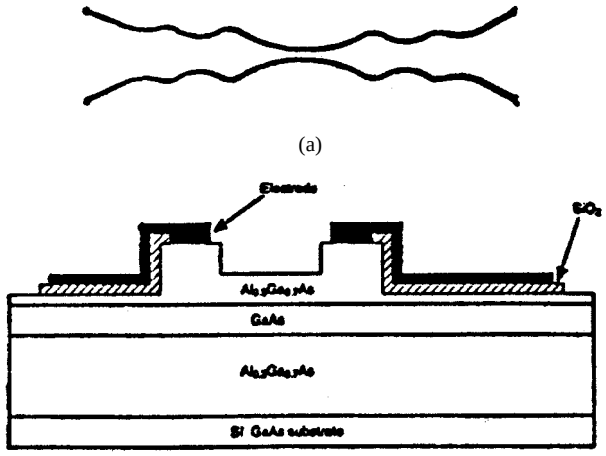

Fig. 6. (a) Top view showing the varying gap between the two waveguides (not drawn to scale). (b) Cross-sectional view of the modulator structure.

where n_e and n_o are the effective indices of the even and the odd supermodes, respectively. The effective index difference between the even and the odd supermodes $(n_e - n_o)$ depends on the interridge gap G for fixed L_{c1}, L_g, L_{c2}, W, H_1, and H_2, and so κ is a function of G. From this we therefore can determine the correlation between the coupling coefficient κ and the interridge gap G; and it was found empirically that

$$G(\text{in } \mu\text{m}) = \frac{1}{0.675} \ln\left[\frac{\pi}{526}\frac{1}{\kappa}\right] \tag{20}$$

where κ has the unit of radian per micrometer in the above equation. Utilizing (20) with κ replaced by $\kappa(z)|_{\text{truncated}}$, which is the actual coupling function that the device will have, we will then get a function $G(z)$, which in fact will give us the "shape" of the modulators we want. Thus we determine the spacing between the two waveguides of the double-ridge structure along its length so as to achieve the desired modulator response function. The devices were designed and fabricated in the Microtechnology Laboratory at the University of Minnesota. The top and the cross-sectional views of the resulting device structure are schematically shown in Fig. 6. The devices thus designed, being 5.1-mm long, have a rather high half-wave voltage (V_π) of 48 V. This is due to the fact that the devices are "short" and that the wide spatially varying gap between the two waveguides in some parts of the device's length gives rise to a very low overlap integral value. Note that V_π is inversely proportional to the product of the overlap integral value and the device length.

V. Experimental Results

A. The DC Response of the Modulator

Before making the dc response measurements on the fabricated devices, we looked at the mode shape of the output beam as well as measured the extinction ratio and the breakdown voltage of the devices. A laser beam of 1.3-μm wavelength was coupled into a polarization-maintaining single-mode fiber, and the beam with TE polarization from the fiber output was coupled into an input arm of the directional-coupler modulator. The far-field optical-mode output from the other arm of the

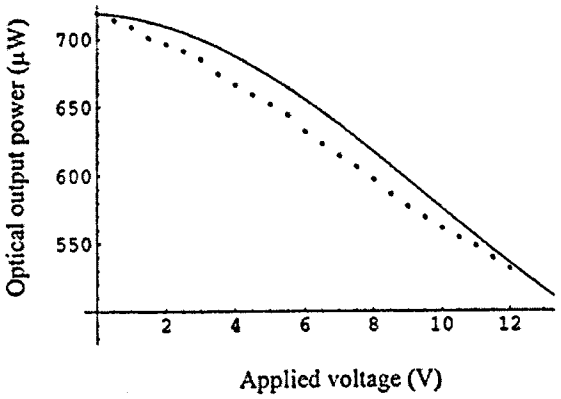

Fig. 7. DC response function of a linearized modulator. Dots—experimental; line—theoretical.

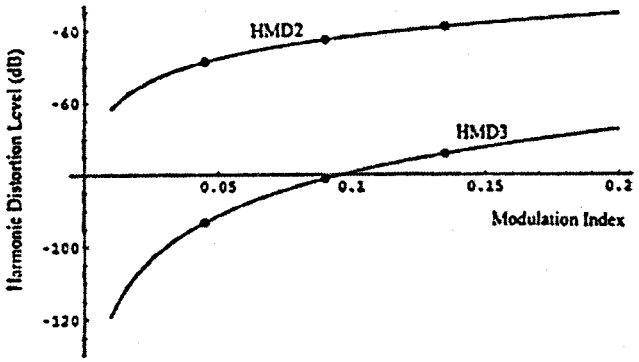

Fig. 8. Second- and third-harmonic distortion levels versus optical modulation index of a linearized modulator.

coupler was then detected using a charge-coupled device (CCD) camera and a monitor. The monitor showed a nice single-mode profile of the beam output from the device.

The extinction ratio was determined by measuring the optical power coming out from each of the two arms of the coupler modulator. The optical output power from the "coupled arm" and the "through arm" of one device was measured to be 774 μW and 18 μW, respectively. The extinction ratio for this device is then 774 μm/18 μm $= 43$, or 16.33 dB.

The breakdown voltage of the devices was measured using a curve tracer. Two probes were connected to the contact pads of the device under test, with each pad connected to the electrode on top of each waveguide ridge. The voltage across the two probes was then increased from zero until the breakdown voltage behavior showed up on the curve-tracer monitor. It was found that the breakdown voltage of two devices under test is both about 17 V. Since this breakdown value is much lower than the half-wave voltage (V_π) of the devices that we designed, which is 48 V, we have to limit the bias voltage applied to the devices under test to be less than 17 V when making the dc response measurement, and for safety reason we took 12 V as a maximum value of the applied bias voltage. Various values of the dc voltage were applied to the electrodes of a linear modulator and the optical output power was measured. The detected optical output power versus the applied voltage (up to 12 V) is plotted in Fig. 7. The theoretically synthesized curve is also included in this figure and has been scaled so that the response at the zero bias coincides with that of the experimental result. We see that the experimental result is fairly close to the theory. The slight discrepancy might stem from the fact that, due to fabrication error, the fabricated devices may not have perfectly the same spatially varying coupling function as that given in the theory.

B. Harmonic Distortions of the Linearized Modulator

A common way to evaluate the linearity of a modulator is to measure harmonic distortions, defined as 10 $\log_{10}$ *[power content of the harmonic/ power content of the fundamental]*, that the device produces under modulation. Plotted in Fig. 8 are the second- and third-harmonic distortion levels versus the optical modulation index of a linearized modulator that we designed and fabricated, biased at 5 V and measured at the fundamental frequency of 500 MHz.

Since the half-wave voltage of this device is 48 V, which is much higher than the breakdown voltage of the device ($\sim$17 V), we could not experimentally bias it at the most linear portion existing somewhere else on the complete response curve; if we could, the second-harmonic distortion level could be minimized and the third-harmonic distortion level would also be simultaneously reduced. Despite the biasing problem, we have got a fairly good experimental result on the third-harmonic distortion level compared to a theoretical result given in the literature [6].

C. Intermodulation Distortions of the Linearized Modulator

When the modulating signal consists of two or more tones, there are intermodulation distortions in addition to harmonic distortions. For narrow-band, or *suboctave*, communication systems, the harmonic distortions and the even-order intermodulation distortions are not a problem as they will be filtered out by the receiver and the system will then be limited by the odd-order intermodulation distortions, of which the *third-order* is the most important as it contains the most power content. In the third-order intermodulation distortion (IMD3) measurements, two pure sinusoidal signals of equal amplitude but slightly different in frequency, in particular, $f_1 = 490$ MHz and $f_2 = 500$ MHz, were combined using a two-way combiner and the output from the combiner was then fed to a bias-T, which was biased at 5 V, and the output from the bias-T was then connected to the electrodes of the device under test. The harmonics generated by the modulator were observed using a spectrum analyzer. Plotted in Fig. 9 is the power content of the fundamental, f_1 or f_2 (top curve), and that of the third-order intermodulation frequency, $(2f_1 - f_2)$ or $(2f_2 - f_1)$ (bottom curve), for various modulator input power. The modulator input power is the drive power from the microwave source times $(1 - |s_{11}|^2)$, where s_{11} is the reflection coefficient of the device at the input port which was measured to be $0.4 + j0.42$ at 500 MHz. For a particular value of the modulator input power, the difference between the top curve and the bottom curve gives the third-order intermodulation distortion (IMD3) level. This measurement was done at the noise bandwidth of 100 Hz and the corresponding noise

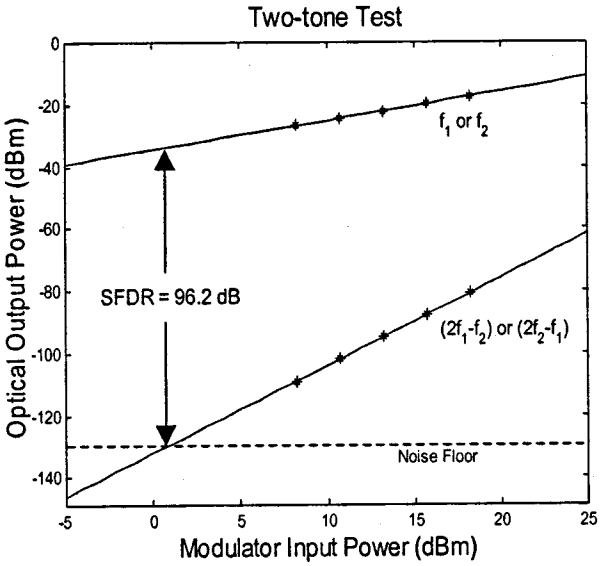

Fig. 9. Third-order intermodulation distortion level versus modulator input power.

floor was -110 dBm, which translates to -130 dBm/Hz. At this noise floor, our linearized modulator exhibits an IMD3-limited spurious-free dynamic range (SFDR) of 96.2 dB/Hz$^{2/3}$.

VI. Conclusion

We used the inverse Fourier transform method as the synthesis technique to obtain the spatially varying coupling function corresponding to an ideal linear-function response of electrooptic directional-coupler modulators. The resulting coupling function was then used to determine the shape of the modulators, built from $Al_{0.3}Ga_{0.7}As/GaAs$ material system and to be operating at the optical wavelength of 1.3 μm. Even though we used an approximate synthesis technique, the resulting devices accordingly designed and fabricated exhibit appreciably higher linearity in their response function than that of generic unlinearized modulators [6], as can be seen from the dc response curve, the third-order harmonic distortion, and the third-order intermodulation distortion. A third-order intermodulation-limited spurious-free dynamic range of 96.2 dB/Hz$^{2/3}$ was obtained. The modulator would show better performance if the full range of voltages could be applied on the electrodes, so that the bias point is on the most linear part of the full response curve. A key to this is to redesign the modulator that has a much lower half-wave voltage (preferably, less than 5 V). Although this is not the best result, it is the first time a linearized electrooptic directional-coupler modulator with a spatially varying coupling function has been built and demonstrated experimentally.

References

[1] L. M. Johnson and H. V. Roussell, "Reduction of intermodulation distortion in interferometric optical modulators," *Opt. Lett.*, vol. 13, no. 10, pp. 928–930, Oct. 1988.

[2] A. Djupsjobacka, "A linearization concept for integrated-optic modulators," *IEEE Photon. Technol. Lett.*, vol. 9, pp. 869–879, Aug. 1992.

[3] M. L. Farwell, Z.-Q. Lin, E. Wooten, and W. S. C. Chang, "An electrooptic intensity modulator with improved linearity," *IEEE Photon. Technol. Lett.*, vol. 3, pp. 792–795, Sept. 1991.

[4] P.-L. Liu, B. J. Li, and Y. S. Trisno, "In search of a linear electrooptic amplitude modulator," *IEEE Photon. Technol. Lett.*, vol. 3, pp. 144–146, Feb. 1991.

[5] H. Skeie and R. V. Johnson, "Linearization of electrooptic modulators by a cascade coupling of phase modulating electrodes," *Integrated Optical Circuits*, vol. SPIE-1583, pp. 153–164, 1991.

[6] W. K. Burns, "Linearized optical modulator with fifth order correction," *J. Lightwave Technol.*, vol. 13, pp. 1724–1727, Aug. 1995.

[7] S. E. Miller, "Coupled wave theory and waveguide applications," *Bell Syst. Tech. J.*, vol. 33, pp. 661–719, 1954.

[8] H. Kogelnik and R. Schmidt, "Switched directional couplers with alternating $\Delta\beta$," *IEEE J. Quantum Electron.*, vol. QE-12, pp. 396–401, July 1976.

[9] R. C. Alferness, "Titanium-diffused lithium niobate waveguide devices," in *Guided-Wave Optoelectronics*, 2nd ed, T. Tamir, Ed. New York: Springer-Verlag, 1990, pp. 145–206.

[10] G.-H. Song and S. Y. Shin, "Design of corrugated waveguide filters by the Gel'fand–Levitan–Marchenko inverse scattering method," *J. Opt. Soc. Amer.*, vol. 2, pp. 1905–1915, Nov. 1985.

[11] K. A. Winick, "Design of grating-assisted waveguide couplers with weighted coupling," *J. Lightwave. Technol.*, vol. 9, pp. 1481–1492, Nov. 1991.

[12] S. W. Løvseth, C. Laliew, and A. Gopinath, "Synthesis of amplitude response of optical directional coupler modulators," in *1997 IEEE MTT-S Int. Microwave Symp. Dig.*, vol. III, June 1997, pp. 1717–1720.

[13] K. A. Winick, "Design of corrugated waveguide filters by Fourier transform techniques," *IEEE J. Quantum Electron.*, vol. 26, pp. 1918–1929, Nov. 1990.

[14] R. C. Alferness and P. S. Cross, "Filter characteristics of codirectionally coupled waveguides with weighted coupling," *IEEE J. Quantum Electron.*, vol. QE-14, pp. 843–847, Nov. 1978.

[15] M. G. Cohen and E. I. Gordon, "Acoustic beam probing using optical techniques," *Bell Syst. Tech. J.*, vol. 44, no. 4, pp. 693–721, Apr. 1965.

[16] S. W. Løvseth, C. Laliew, and A. Gopinath, "Amplitude response of optical directional coupler modulators by Fourier transform technique," in *8th Eur. Conf. Integrated Optics Proc.*, Stockholm, Sweden, Apr. 1997, pp. 230–233.

[17] E. Gamire, "Semiconductor components for monolithic applications," in *Topics in Applied Physics*, T. Tamir, Ed. New York: Springer-Verlag, 1979, vol. 7, pp. 244–304.

[18] K. L. Johnson, "Nonuniform semi-vectorial finite difference analysis of dielectric waveguide structure," Master's degree thesis, Univ. Minnesota, Minneapolis, 1993.

[19] M. H. Khan, "Electrooptic waveguide directional coupler modulator in aluminum arsenide–gallium arsenide," Ph.D. dissertation, Univ. Minnesota, Minneapolis, 1994.

[20] H. Nishihara, M. Haruna, and T. Suhara, *Optical Integrated Circuits*. New York: McGraw-Hill, 1989.

[21] K. K. Loi, J. H. Hodiak, X. B. Mei, C. W. Tu, and W. S. C. Chang, "Linearization of 1.3 μm MQW electro-absorption modulators using an all-optical frequency-insensitive technique," *IEEE Photon. Technol. Lett.*, vol. 10, pp. 964–966, July 1998.

Chanin Laliew was born in Bangkok, Thailand, in 1971. He received the B.S. and M.S. degrees in electrical engineering from the University of Minnesota in 1995 and 1999, respectively. He is currently pursuing the Ph.D. degree in the same field at the same university.

His research interests include optoelectronics and wireless and fiber-optic communication systems.

Sigurd Weidemann Løvseth, photograph and biography not available at the time of publication.

Xiaboo Zhang, photograph and biography not available at the time of publication.

Anand Gopinath (S'64–M'65–SM'80–F'90), photograph and biography not available at the time of publication.